

# Dielectric in Waveguide cavity analysis

Corwin Shiu

April 27, 2017

*The purpose of this document is to provide an theoretical analysis of a partially filled waveguide cavity with a dielectric. This analysis will inform how to best do a measurement of dielectric loss and dielectric. The analysis in this document follows from Robert E Collins, Field Theory of Guided Waves 2nd ed. in the chapter Inhomogeneously Filled Waveguides and Dielectric Resonators. I'll elaborate on the actual modal structure in the rectangular waveguides, and extend the analysis to cavities.*

## 1 Partially filled rectangular waveguide



Figure 1: Two types of filling geometries (a) side filled, (b) bottom filled.

The introduction of a dielectric in a rectangular waveguide changes the type of propagating modes. Modes in a dielectric filled waveguide are transverse electric or transverse magnetic. With the introduction of an interface, the fundamental modes are hybrid modes, characterized by the lack of  $\vec{E}$  field normal to the dielectric interface, called **longitudinal section electric (LSE) mode**, or by the lack of  $\vec{H}$  field normal to the interface called **longitudinal section magnetic (LSM) mode**. We can make sense of this from figure 2. Because we're going to eventually couple our partially filled waveguide with a regular bare waveguide operating with a  $TE_{10}$  mode, we don't have to do the full analysis. We only need to look at LSE modes for type (1a) and LSM modes for type (1b).

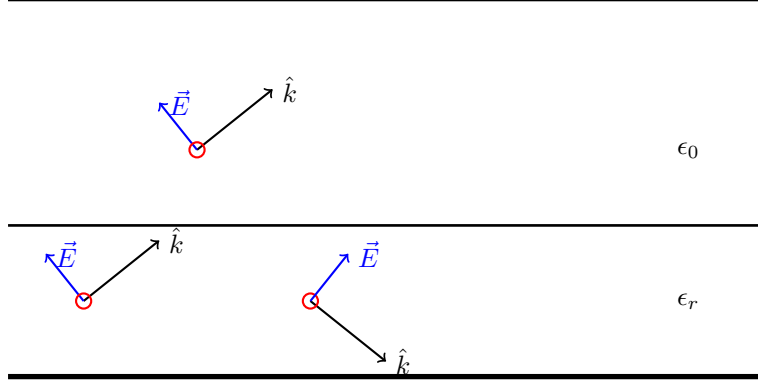


Figure 2: An intuitive explanation for why partially filled waveguides lack transverse modes. Internal reflection inside the dielectric is pictured here, for the waveguide geometry shown in figure (1b). Matching the electric field at the dielectric boundary would force  $\vec{E}$  in the  $\hat{z}$  direction, so we cannot have transverse electric or magnetic fields. If we have total internal reflection, then the fields in vacuum would be evanescent.

### 1.1 Longitudinal section electric (LSE) Modes

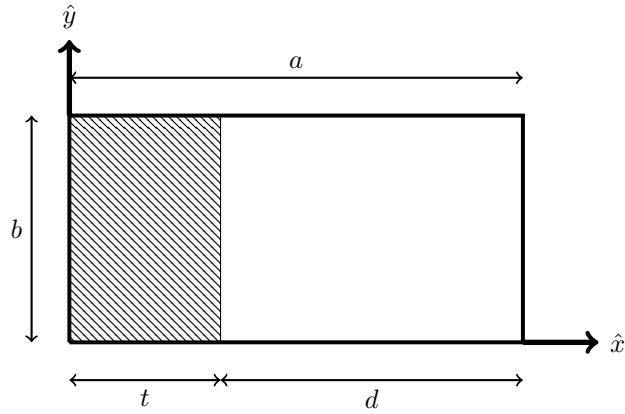


Figure 3: Asymmetrical dielectric slab-loaded waveguide. This geometry is studied in this section.

**Analytic Results** For the LSE mode, we need to find the magnetic Hertzian potential. Because the dielectric is placed normal to  $\hat{x}$ , the potential has the form  $\Pi_h = \hat{x}\psi_h(x, y)e^{-j\beta z}$  with the corresponding fields,

$$\begin{aligned}\vec{E} &= -j\omega\mu_0\nabla \times \Pi_h \\ \vec{H} &= \nabla \times \nabla \times \Pi_h\end{aligned}$$

and the Hertz potential solves the wave equation,

$$\nabla^2\Pi_h + k^2\Pi_h = \left(\frac{\partial^2}{\partial x^2} + \frac{\partial^2}{\partial y^2} + (\kappa(x)k_0 - \beta^2)\right)\psi_h(x, y) = 0$$

where,

$$\kappa(x) = \begin{cases} \epsilon_r & 0 \leq x < t \\ 1 & t < x \leq a \end{cases}$$

A solution to the differential equation is of the form,

$$\psi_h = \begin{cases} A \sin \ell x \cos \frac{m\pi y}{b} & 0 \leq x < t \\ B \sin h(a-x) \cos \frac{m\pi y}{b} & t < x \leq a \end{cases}$$

and the relationship between the wavenumbers in the two regions ( $h, \ell$ ) are related by,

$$-\beta^2 = \ell^2 + \left(\frac{m\pi}{b}\right)^2 - \epsilon_r k_0^2 = h^2 + \left(\frac{m\pi}{b}\right)^2 - k_0^2 \quad (1)$$

This condition is apparent if we plug in our ansatz for the two regions, and enforcing that the propagation constant of the mode  $\beta$  is the same in both regions (otherwise it wouldn't be a normal mode!). We will now show how this ansatz satisfies the boundary conditions (that  $E_{\parallel} = 0, H_{\perp} = 0$  for metallic surfaces). The electric field dropping off constants for the region inside the dielectric

$$E_{<} = -j\omega\mu_0 \begin{bmatrix} \hat{x} & \hat{y} & \hat{z} \\ \frac{\partial}{\partial x} & \frac{\partial}{\partial y} & \frac{\partial}{\partial z} \\ A \sin \ell x \cos \frac{m\pi y}{b} e^{-j\beta z} & 0 & 0 \end{bmatrix} \propto -j\beta \sin \ell x \cos \frac{m\pi y}{b} e^{-j\beta z} \hat{y} - \frac{m\pi}{b} \sin \ell x \sin \frac{m\pi y}{b} e^{-j\beta z} \hat{z}$$

We see that  $E_y = 0$  and  $E_z = 0$  at the boundary  $x = 0$ , so we have no electric fields parallel to the side walls. Additionally  $E_z = 0$  at the base  $y = 0$ , so there's no electric fields parallel to the base. Now for  $H$  fields,

$$H_{<} = \nabla \times \begin{bmatrix} \hat{x} & \hat{y} & \hat{z} \\ \frac{\partial}{\partial x} & \frac{\partial}{\partial y} & \frac{\partial}{\partial z} \\ A \sin \ell x \cos \frac{m\pi y}{b} e^{-j\beta z} & 0 & 0 \end{bmatrix} \propto \begin{bmatrix} \hat{x} & \hat{y} & \hat{z} \\ \frac{\partial}{\partial x} & \frac{\partial}{\partial y} & \frac{\partial}{\partial z} \\ 0 & \sin \ell x \cos \frac{m\pi y}{b} e^{-j\beta z} & \sin \ell x \sin \frac{m\pi y}{b} e^{-j\beta z} \end{bmatrix} \\ \propto \hat{x} \left( \frac{m\pi}{b} \sin \ell x \cos \frac{m\pi y}{b} e^{-j\beta z} - j\beta \sin \ell x \cos \frac{m\pi y}{b} e^{-j\beta z} \right) + \hat{y} \left( \ell \cos \ell x \sin \frac{m\pi y}{b} e^{-j\beta z} \right) + \hat{z} \left( \ell \cos \ell x \cos \frac{m\pi y}{b} e^{-j\beta z} \right)$$

So  $H_x$  disappears when  $x = 0$ ,  $H_y$  disappears when  $y = 0, b$ . So we have no magnetic fields perpendicular to the waveguide boundary. The condition at  $x = a$  can be repeated,

$$E_{>} = -j\omega\mu_0 \begin{bmatrix} \hat{x} & \hat{y} & \hat{z} \\ \frac{\partial}{\partial x} & \frac{\partial}{\partial y} & \frac{\partial}{\partial z} \\ B_{>} \sin h(a-x) \cos \frac{m\pi y}{b} e^{-j\beta z} & 0 & 0 \end{bmatrix} \propto -j\beta \sin h(a-x) \cos \frac{m\pi y}{b} e^{-j\beta z} \hat{y} - \frac{m\pi}{b} \sin h(a-x) \sin \frac{m\pi y}{b} e^{-j\beta z} \hat{z}$$

which we immediately see that at  $x = a$ ,  $E_y = 0, E_z = 0$ . For the magnetic field,

$$H_{>} = \nabla \times \begin{bmatrix} \hat{x} & \hat{y} & \hat{z} \\ \frac{\partial}{\partial x} & \frac{\partial}{\partial y} & \frac{\partial}{\partial z} \\ B \sin h(a-x) \cos \frac{m\pi y}{b} e^{-j\beta z} & 0 & 0 \end{bmatrix} \propto \begin{bmatrix} \hat{x} & \hat{y} & \hat{z} \\ \frac{\partial}{\partial x} & \frac{\partial}{\partial y} & \frac{\partial}{\partial z} \\ 0 & \sin h(a-x) \cos \frac{m\pi y}{b} e^{-j\beta z} & \sin h(a-x) \sin \frac{m\pi y}{b} e^{-j\beta z} \end{bmatrix} \\ \propto \hat{x} \left( \frac{m\pi}{b} \sin h(a-x) \cos \frac{m\pi y}{b} e^{-j\beta z} - j\beta \sin h(a-x) \cos \frac{m\pi y}{b} e^{-j\beta z} \right) + \hat{y} \left( -h \cos h(a-x) \sin \frac{m\pi y}{b} e^{-j\beta z} \right) \\ + \hat{z} \left( -h \cos h(a-x) \cos \frac{m\pi y}{b} e^{-j\beta z} \right)$$

so  $H_y$  disappears when  $x = a$  and  $H_z$  disappears when  $y = 0, b$ . So this ansatz fully satisfies the boundary conditions at the walls of the waveguide.

Now we have to impose the continuity expressions at  $x = t$ .  $E_z$  must be continuous and  $H_y$  is continuous,

$$A \sin \ell t = B \sin h d \\ A \ell \cos \ell t = -B h \cos h d$$

which we can eliminate the constants by dividing the equations together,

$$h \tan \ell t = -\ell \tan h d \quad (2)$$

Equation 1 and equation 2 together is the key to finding the modal structure. Before we plug these equations into Matlab to mindlessly churn, there's physical insight to keep in mind or you'll miss key physical features of this system.

**Key features of analytic expressions**

- i  $\ell$  and  $h$  are the wavenumbers in the dielectric and air region of the waveguide.
- ii  $h$  is allowed to be real *or* imaginary.
- iii A real  $h$  indicates propagation of power in both the dielectric and air regions.
- iv An imaginary  $h$  has power propagating along the dielectric only, with evanescent modes in the air region. This is just like an optical fiber.
- v Even if we have a solution to the transcendental equation, the mode may not propagate. We have to check whether  $\beta$  is real or imaginary.
- vi Modes with  $m = 0$  look like  $TE_{n0}$  modes.

**Example** We can take one example to illustrate the solution process. Figure 4 illustrates the modes in the waveguide in  $k$ -space, marked by the zeros of the function. The numerical values are inspired by WR-10. We study a guide with  $a = 2.54mm, b = 1.27mm$  with a  $0.5mm$  thick  $\epsilon_r = 4$  dielectric. We study the system at 2 frequencies at  $f_0 = 100, 200GHz$ . The plot of equation 2 rearranged to be,

$$f(l) = h \tan(\ell(h)t) + \ell(h) \tan(hd)$$

The contour plot underneath the plot is the real value of  $\beta$  from equation 1. Blue indicates no real part to  $\beta$ , indicating that the solution is imaginary and therefore the modes don't propagate.

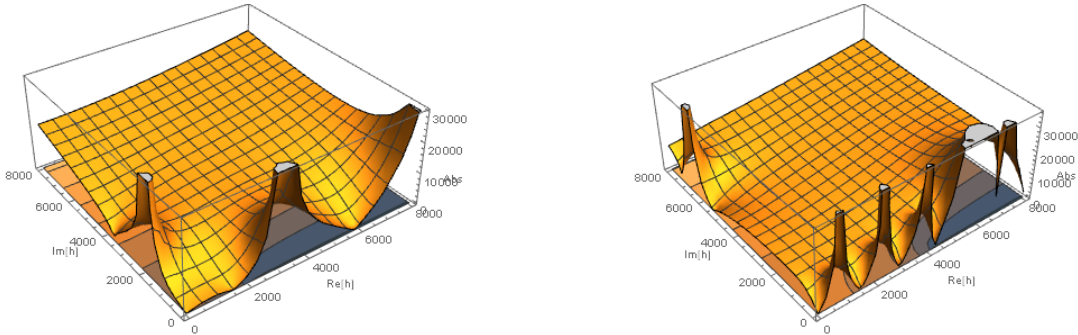


Figure 4: The zeros of the function illustrates modes in rectangular waveguide with top being 100GHz and bottom being at 200GHz.

Solutions with purely imaginary  $h$  have waves of total internal reflection at the boundary, so the modes are evanescent in air. Solutions with purely real  $h$  have propagating waves in both the dielectric and in air. At low frequencies, only dielectric modes propagate, illustrated by being the only allowed mode in the upper 100GHz plot. At high frequencies, in the bottom 200GHz plot, we have two dielectric modes and two hybrid modes that are allowed to propagate.

**HFSS Confirmation** We can simulate this easily in HFSS. We illustrate two modes. In this document, I'm not going to bother with showing the analytical fields, but it's easy to do. It's important to carry all the numerical constants in order for the fields to match at the two boundaries.

**Take-away points** The reason you should pay attention to this is because this informs how the waveguide cavity should be set up. This analysis shows that we in fact have modes with  $\vec{E}$  that has the appearance of rectangular TE modes (although the  $\vec{H}$  fields don't look nearly the same), which indicate we can in principal feed a waveguide cavity efficiently. However the analysis also shows certain modes are hopeless to drive - the dielectric modes of type (a) will be hopeless to drive even though they are the first modes to be allowed to propagate in the guide. Figure 5b instead would be much more natural to drive but is counterintuitive purely looking at  $s$ -parameters because these are high order modes in this waveguide.

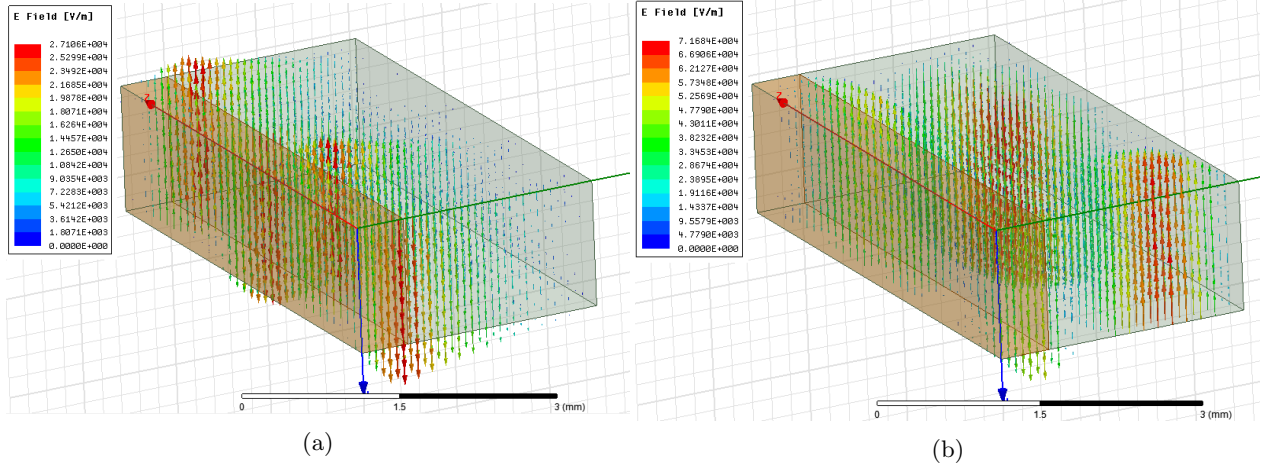


Figure 5:  $\vec{E}$  field distributions of simulated waveguide modes. (a) shows the fundamental mode, with power propagating along the dielectric and evanescent in air. (b) shows propagation of the hybrid mode in both air and dielectric. The simulated cutoffs are 84GHz and 107GHz respectively, in agreement with numerical results.

## 1.2 Longitudinal section magnetic (LSM) Modes

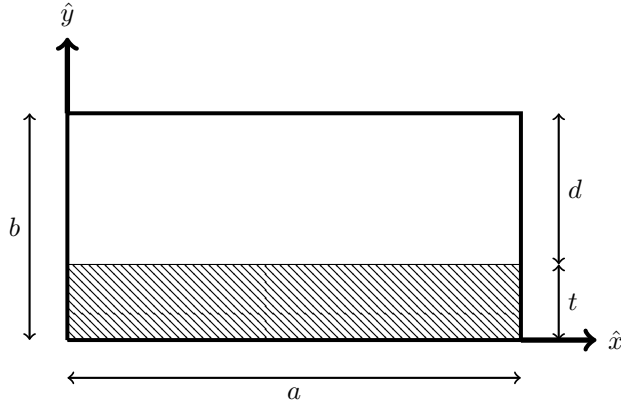


Figure 6: Asymmetrical dielectric slab-loaded waveguide. This geometry is studied in this section.

**Analytic Results** For the LSM modes, we need an electric Hertzian potential. Because the dielectric is placed normal to  $\hat{y}$ , the potential has the form,  $\Pi_e = \hat{y}\psi_e(x, y)e^{-j\beta z}$ , with the corresponding fields,

$$\begin{aligned} H &= j\omega\epsilon_0\kappa(y)\nabla \times \Pi_e \\ E &= \nabla \times \nabla \times \Pi_e \end{aligned}$$

and the Hertzian potential solves the wave equation,

$$\nabla^2\Pi_e + k^2\Pi_e = \left( \frac{\partial^2}{\partial x^2} + \frac{\partial^2}{\partial y^2} + (\kappa(y)k_0 - \beta^2) \right) \psi_e(x, y) = 0$$

where,

$$\kappa(y) = \begin{cases} \epsilon_r & 0 \leq y < t \\ 1 & t < y \leq b \end{cases}$$

A solution to the differential equation is of the form,

$$\psi_e = \begin{cases} A \sin \frac{n\pi x}{a} \cos \ell y & 0 \leq y < t \\ B \sin \frac{n\pi x}{a} \cos h(b-y) & t < y \leq b \end{cases}$$

and we get the same relationship from plugging in this ansatz in the wave equation,

$$-\beta^2 = \ell^2 + \left(\frac{n\pi}{a}\right)^2 - \epsilon_r k_0^2 = h^2 + \left(\frac{n\pi}{a}\right)^2 - k_0^2 \quad (3)$$

Now we're going to show that this ansatz satisfies boundary conditions that  $E_{\parallel} = 0$  and  $H_{\perp} = 0$  along the boundary of the waveguide. Inside the dielectric,

$$H_{<} = j\omega\epsilon_r\epsilon_r \begin{bmatrix} \hat{x} & \hat{y} & \hat{z} \\ \frac{\partial}{\partial x} & \frac{\partial}{\partial y} & \frac{\partial}{\partial z} \\ 0 & A \sin \frac{n\pi x}{a} \cos \ell y e^{-j\beta z} & 0 \end{bmatrix} \propto -\hat{x}j\beta \sin \frac{n\pi x}{a} \cos \ell y e^{-j\beta z} + \hat{z} \frac{n\pi}{a} \cos \frac{n\pi x}{a} \cos \ell y e^{-j\beta z}$$

At the boundaries  $x = 0, a$ , the magnetic field  $H_x = 0$  so that there is no magnetic field perpendicular to the side walls. At  $y = 0$ , there is no  $H_y$  so no magnetic field is perpendicular to the base.

$$E_{<} = \nabla \times \nabla \times \Pi_e = \begin{bmatrix} \hat{x} & \hat{y} & \hat{z} \\ \frac{\partial}{\partial x} & \frac{\partial}{\partial y} & \frac{\partial}{\partial z} \\ -j\beta \sin \frac{n\pi x}{a} \cos \ell y e^{-j\beta z} & 0 & \frac{n\pi}{a} \cos \frac{n\pi x}{a} \cos \ell y e^{-j\beta z} \end{bmatrix}$$

$$= \hat{x} \left( -\frac{n\pi}{a} \ell \cos \frac{n\pi x}{a} \sin \ell y e^{-j\beta z} \right) + \hat{y} \left( \beta^2 \sin \frac{n\pi x}{a} \cos \ell y e^{-j\beta z} - \frac{n^2 \pi^2}{a^2} \sin \frac{n\pi x}{a} \cos \ell y e^{-j\beta z} \right) + \hat{z} \left( \beta \ell \sin \frac{n\pi x}{a} \sin \ell y e^{-j\beta z} \right)$$

We can see that at the boundaries  $x = 0, a$ , both  $E_x = 0, E_y = 0$  so there is no electric fields parallel to the side walls. The base  $y = 0$ , there is also no  $E_z = 0$ , so all boundary conditions in the dielectric portion is fulfilled. We can repeat the analysis for the top.

$$H_{>} = j\omega\epsilon_0 \begin{bmatrix} \hat{x} & \hat{y} & \hat{z} \\ \frac{\partial}{\partial x} & \frac{\partial}{\partial y} & \frac{\partial}{\partial z} \\ 0 & B \sin \frac{n\pi x}{a} \cos h(b-y) e^{-j\beta z} & 0 \end{bmatrix} \propto -\hat{x}j\beta \sin \frac{n\pi x}{a} \cos h(b-y) e^{-j\beta z} + \hat{z} \frac{n\pi}{a} \cos \frac{n\pi x}{a} \cos h(b-y) e^{-j\beta z}$$

at the boundary  $y = b$  there is no  $H_y$  fields so we satisfy the boundary condition of the top wall. As  $x = 0, a$ , the term  $H_x = 0$ , so we have no perpendicular  $H$  fields in the upper portion.

$$E_{>} = \nabla \times \nabla \times \Pi_e = \begin{bmatrix} \hat{x} & \hat{y} & \hat{z} \\ \frac{\partial}{\partial x} & \frac{\partial}{\partial y} & \frac{\partial}{\partial z} \\ -j\beta \sin \frac{n\pi x}{a} \cos h(b-y) e^{-j\beta z} & 0 & \frac{n\pi}{a} \cos \frac{n\pi x}{a} \cos h(b-y) e^{-j\beta z} \end{bmatrix}$$

$$= \hat{x} \left( -\frac{n\pi}{a} h \cos \frac{n\pi x}{a} \sin h(b-y) e^{-j\beta z} \right) + \hat{y} \left( -\frac{n^2 \pi^2}{a^2} \sin \frac{n\pi x}{a} \cos h(b-y) e^{-j\beta z} + \beta^2 \sin \frac{n\pi x}{a} \cos h(b-y) e^{-j\beta z} \right)$$

$$\hat{z} \left( j\beta h \sin \frac{n\pi x}{a} \sin h(b-y) e^{-j\beta z} \right)$$

From this expression we see that at  $y = b$ , the electric fields  $E_x, E_z = 0$  so there is no parallel electric fields to the top boundary. At  $x = 0, x = a$  the field  $E_y = 0$  so there is no parallel electric field to the side walls. All boundary conditions are met with this ansatz.

Now we have to impose the continuity expressions at  $y = t$ .  $E_x$  must be continuous and  $H_z$  is continuous,

$$A \ell \sin \ell t = B h \sin h d$$

$$-A \epsilon_r \cos \ell t = B \sin h d$$

if we divide the two equations, we obtain a transcendental equation,

$$-\ell \tan \ell t = \epsilon_r h \tan h d \quad (4)$$

Equation 3 and equation 4 together is the key to finding the modal structure. Just like the LSE analysis we have done above, there's physical insight to keep in mind or you'll miss key physical features of this system.

### Key features of analytic expressions

- i  $\ell$  and  $h$  are the wavenumbers in the dielectric and air region of the waveguide.
- ii  $h$  is allowed to be real *or* imaginary.
- iii A real  $h$  indicates propagation of power in both the dielectric and air regions.
- iv An imaginary  $h$  has power propagating along the dielectric only, with evanescent modes in the air region. This is just like an optical fiber.
- v Even if we have a solution to the transcendental equation, the mode may not propagate. We have to check whether  $\beta$  is real or imaginary.
- vi Modes with  $n = 1$  are the lowest order modes. There is no corresponding mode to a unloaded rectangular waveguide.

**Example** We can take one example to illustrate the solution process, and the method parallels the one outlined in LSE mode. We plot the function 4 in  $h$  space (which is  $k$ -space for the upper portion of the waveguide). The zeros mark the modes. We use dimensions inspired by WR-10 with  $a = 2.54mm, b = 1.27mm$ , a  $0.05mm$  thick  $\epsilon_r = 4$  dielectric. We analyze the system at two frequencies  $f_0 = 100, 200GHz$ .

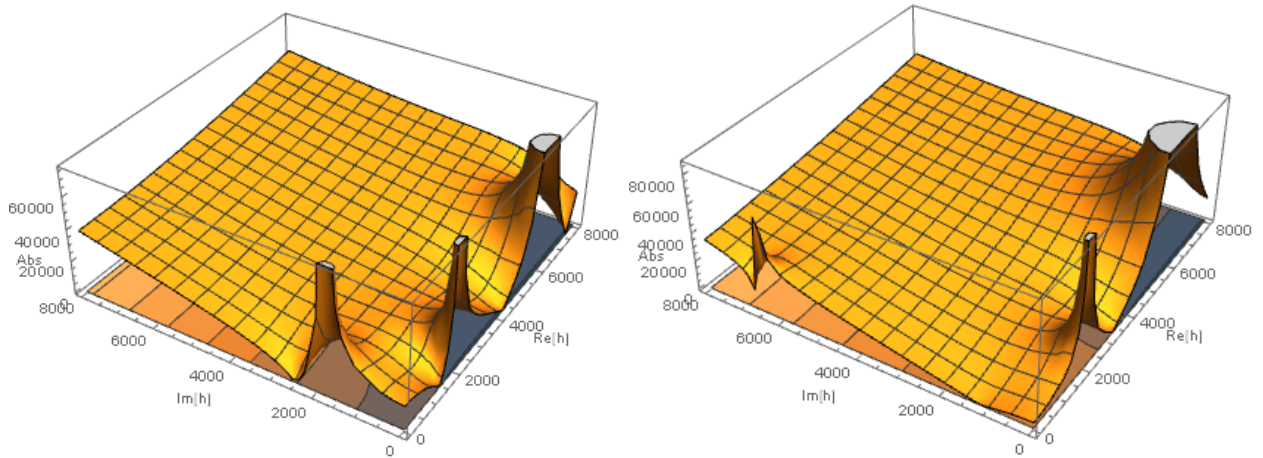


Figure 7: The zeros of the functions illustrates modes in the rectangular waveguide that is bottom loaded with a dielectric slab. Left shows 100GHz while right is 200GHz.

There is one solution with purely imaginary  $h$  corresponding to modes of total internal reflection inside the dielectric. The modes with purely real  $h$  corresponds to propagating modes in both media. The contour plot in blue shows the real part of  $\beta$ . At 100GHz only the evanescent mode propagates but at higher frequency there are two dielectric modes and one hybrid mode.

**HFSS Confirmation** We can simulate this geometry easily in HFSS. We illustrate three modes. However the first two modes correspond to the zero near  $h = 2560j$ , and differ because  $n = 1$  and  $n = 2$ . The third mode has  $h = 1380, n = 1$ .

**Take away points** This analysis shows that at low frequency modes are non-ideal to couple to  $TE_{10}$ . At high frequencies, we have modes that are quasi- $TE_{n0}$  (like in figure 8c).  $\vec{E}$  fields will point in the  $\hat{y}$  direction, but also have non-zero  $E_x$  components. This suggests that if we make a waveguide cavity, coupling with the  $TE_{10}$  mode, we will see more defined resonant features in the high frequency range. However because the fields are not exactly  $TE_{10}$ , we will not get perfect coupling on resonance. Contrast this with the previous analysis where the low order modes behave exactly like  $TE_{n0}$ . This analysis suggests the side loaded dielectric would provide a cleaner signal.

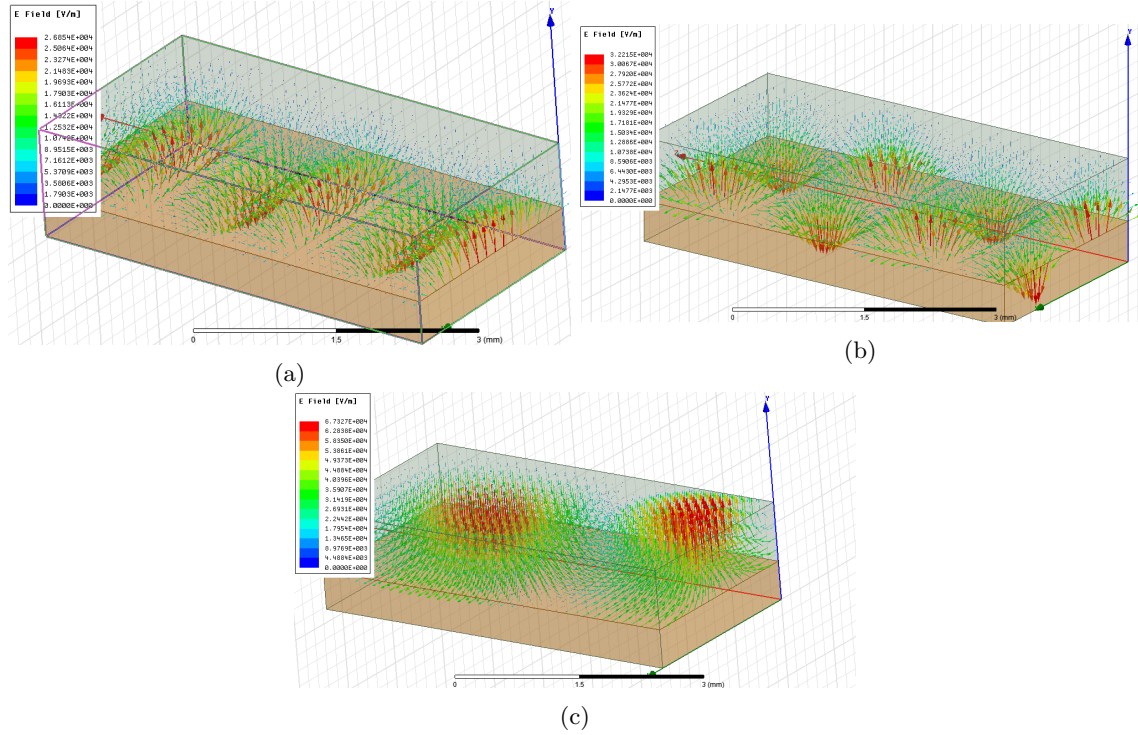
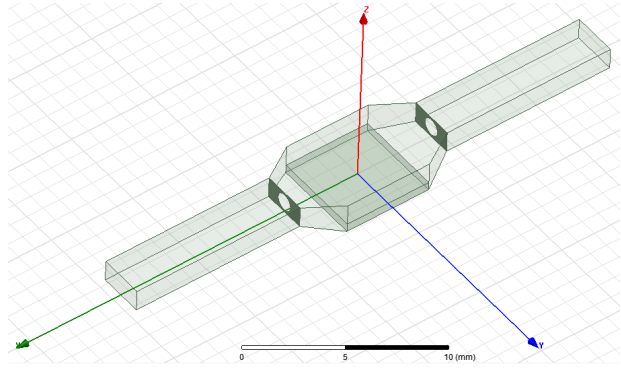


Figure 8:  $\vec{E}$  field distributions of simulated waveguide modes. (a) shows the fundamental mode, with power propagating along the dielectric and evanescent in air. The lowest mode is  $n = 1$ . (b) shows the next mode, which is the next dielectric mode. It has the same purely imaginary  $h$  as (a), but is  $n = 2$ . (c) shows a hybrid propagation mode

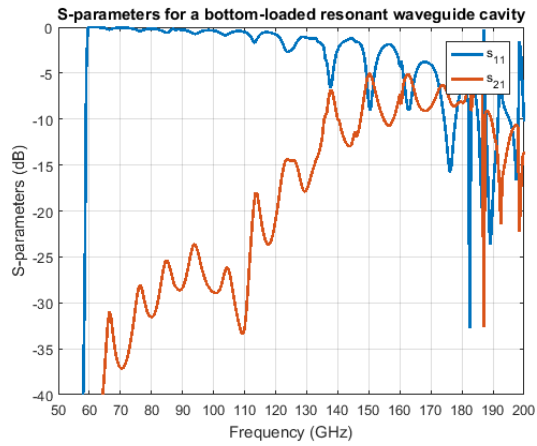
## 2 Waveguide Cavity setup

### 2.1 Bottom Filled dielectric

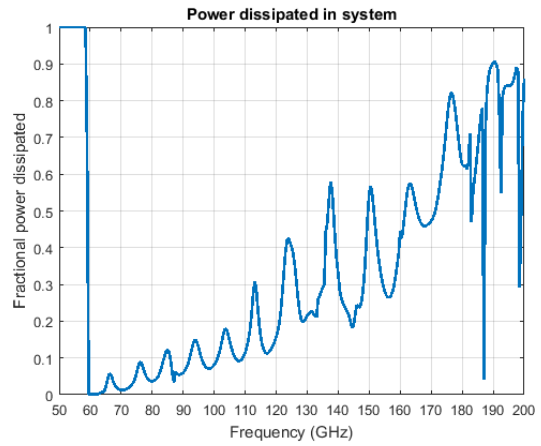
### 2.2 Side filled dielectric



(a)

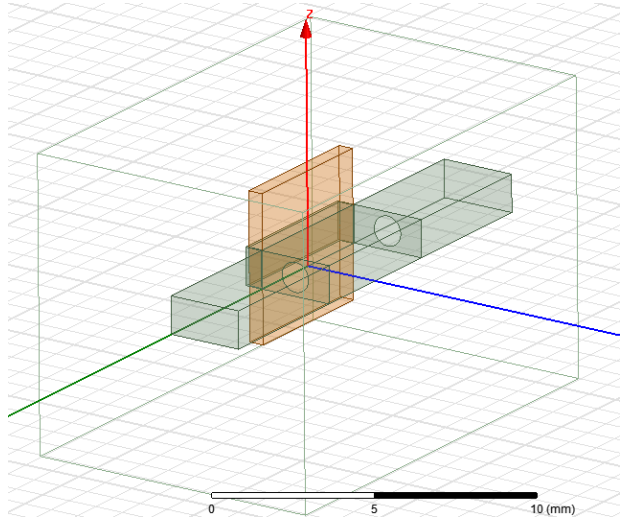


(b)

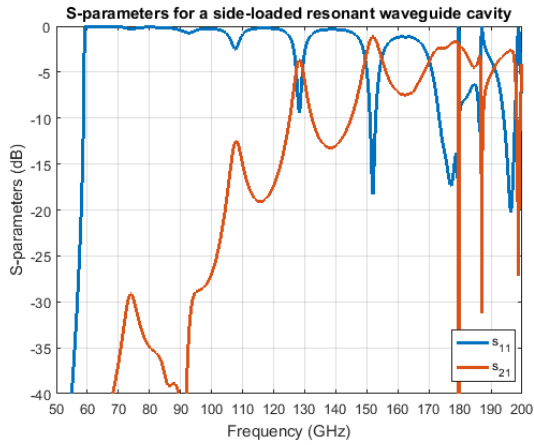


(c)

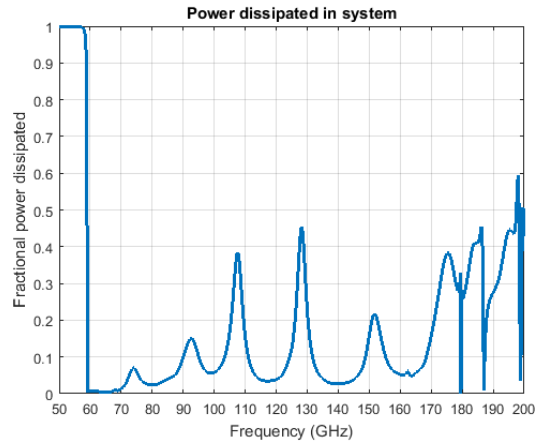
Figure 9: (a) geometry of the simulation with corresponding (b) S-parameters and (c) power absorbed by the dielectric. We see that more power is dissipated in the dielectric at higher frequencies, because higher frequency modes are more aligned with the  $TE_{10}$  mode, so more power is injected into the cavity.



(a)



(b)



(c)

Figure 10: (a) geometry of the simulation with corresponding (b) S-parameters and (c) power absorbed by the dielectric. Because we have a small cavity with the  $TE_{n0}$  mode in band, we get a clean signal. The difficulty is figuring out whether dissipation from the microwave cavity is through dielectric or through radiative losses.